

*Full Length Research Paper*

# Physical properties of active site of tubulin–binding as anticancer nanotechnology investigation

M. Monajjemi<sup>1</sup>, L.Saedi<sup>2</sup>, F. Najafi<sup>2</sup> and F. Mollaamin<sup>1\*</sup>

<sup>1</sup>Department of Chemistry, Science and Research Branch, Islamic Azad University, Tehran, Iran

<sup>2</sup>Science and Research Branch, Islamic Azad University, Tehran, Iran.

Accepted 13 July, 2010

The discovery of numerous tubulin–binding anticancer agents raises the question of how and where the different agents bind on tubulin affect their antimitotic property. Antimitotic of vinblastine families binding site inhibit microtubule assembly. The ultimate action of this agent causes mitotic arrest by inhibiting normal dynamic instability at very low concentration. The investigation of vinblastine has been studied by theoretical methods. It has been established as the best structural and functional of vinblastine. In an effort to understand the conformational preferences that may be attributed to stereoelectronic effects, a number of computational chemistry studies carried out. Molecular mechanics, Monte Carlo, Molecular Dynamics and Langevin calculations have been performed on vinblastine. These results show the minimized structure of vinblastine, calculated potential energy for important dihedral angles and the effect of temperature on geometry of optimized structure. However, the vinblastine compound has been displayed different spectrum of gas phase and solvent NMR by GIAO and CSGT approximations, which appears the results of the determination of the number of active sites in vinblastine using the Onsager method that the O29 has the most shifting at indicated model and it has been reflected mostly the transfer of vinblastine to a less polar environment. These simulations provide an atomistic analysis of the vinblastine strategy and its implications for further investigations of microtubule.

**Key words:** Vinblastine, Monte Carlo, molecular dynamic, Langevin dynamic, NMR, DFT.

## INTRODUCTION

Medicinal chemistry depends on many other disciplines ranging from organic chemistry and pharmacology to computational chemistry. Typically medicinal chemists use the most straightforward ways to prepare compounds. The validation of any design project comes from the biological testing. Cancer is a general term used to describe many disease states, each of which are characterized by abnormal cell proliferation. The causes which bring about this abnormal cellular behavior are specific to each type of cancer.

Derivatives of vinca alkaloids including vinblastine, vincristine and more recently, vinorelbine are effective in studies of cancer chemotherapy (Lobert et al., 2007, 1999, 1996, 2000, 1998; Lee et al., 1975; Correia and

Lobert, 2001; Desai and Mitchison, 1997; VanBuren et al., 2005; Bunt, 1973; Lobert and Correia, 2000; Rai and Wolff, 1996) yet the molecular origins of their differential antitumor and toxic side effects remain uncertain. They cause mitotic arrest by interacting with tubulin heterodimers and mitotic spindle microtubules. Vinca alkaloids inhibit the polymerization of tubulin into microtubules and it has been suggested that *in vivo* vincas act at the ends of microtubules and diminish an essential aspect of cell division, dynamic instability (Lobert et al., 2007, 1999; Lee et al., 1975). Vinca alkaloids produce their antitumor effects by halting cell division at metaphase. These drugs *in vivo* interact with free tubulin and with tubulin in mitotic spindles causing spiral formation and diminished microtubules' dynamic instability (Lobert et al., 1999).

The goal of work described here was to evaluate and quantify the molecular basis for relative stability of

\*Corresponding author. E-mail: [smollaamin@gmail.com](mailto:smollaamin@gmail.com).

vinblastine in water, methanol and ethanol solvents.

Molecular mechanic simulation method are specially useful in studying systems with a large number of coupled degrees of freedom, such as liquids disordered materials, strongly coupled solids and cellular structures. These methods are very important in physical chemistry particularly for simulations involving atomic clusters (Haile and Wiley, 1991; Allan and Tildesley, 1987; van Gunsteren and Berendsen, 1990; Longman, 1996; Frenkel and Smith, 2002). The aim of this work is to understand molecular mechanic of vinblastine drug, which will be useful for designing anticancer drugs. Here in we used molecular mechanic simulation, within the Monte Carlo (MC), Molecular Dynamics (MD) and Langevin Dynamic (LD) approaches. In this study we extract structure information of vinblastine and some thermodynamic parameters and energy of vinblastine in different temperature from this method. The results indicate good agreement in all of the methods.

Also, the information gathered in this investigation from the atomic structure of tubulin involved dynamic instability of microtubules, gives additional help in determining crucial binding site for the activity of potent antimetabolic drugs.

## SIMULATION PROCEDURES

Biologically processes also occur in solution, aqueous systems with rather specific pH and ionic conditions. Most reactions are both qualitatively and quantitatively different under gas and solution phase conditions, especially those involving ions or polar species (Monajjemi et al., 2009).

Molecular properties are also sensitive to the environment. Simulations are therefore intimately related with describing solute-solvent interactions, but such effects can also be modeled with less rigorous methods.

For most notable liquids and solutions systems, the macroscopic quantities derived from the partition function must be estimated from a representative sampling of the phase space. Simulation refers to methods aimed at generating a representative sampling of a system at a finite temperature (Haile and Wiley, 1991; Allan and Tildesley, 1987; van Gunsteren and Berendsen, 1990; Longman, 1996; Frenkel and Smith, 2002).

### Monte-Carlo method

Monte-Carlo simulations are widely used in the fields of chemistry, biology, physics and engineering in order to determine the structural and thermodynamic properties of complex systems at the atomic level. Thermodynamic averages of molecular properties can be determined from Monte Carlo methods, as can minimum-energy structures (Monajjemi and Chahkandi, 2004, 2006, 2008).

In Monte Carlo (MC) methods (Jorgensen, 1988), a sequence of points in phase space is generated from an initial geometry by adding a random "kick" to the coordinates of a randomly chosen particle (atom or molecule). The new configuration is accepted if the energy decreases and with a probability of  $e^{-\Delta E/kT}$  if the energy increases. This Metropolis procedure (Metropolis et al., 1953) ensures that the configurations in the ensemble, obey a Boltzmann distribution and the possibility of accepting higher energy configurations allows MC methods to climb uphill and escape from

a local minimum.

MC simulations require only the ability to evaluate the energy of the system, which may be advantageous if calculating the first derivative is difficult or time-consuming. Furthermore, since only a single particle is moved in each step, only the energy changes associated with this move must be calculated, not the total energy for the whole system. A disadvantage of MC methods is the lack of the time dimension and atomic velocities and they are therefore not suitable for studying time-dependent phenomena or properties depending on momentum (Monajjemi et al., 2008; Haeri et al., 2009).

### Molecular dynamics method

Molecular Dynamics (MD) methods generate a series of time-correlated points in phase space (a trajectory) by propagating a starting set of coordinates and velocities according to Newton's second equation by a series of finite time steps. Unlike single point and geometry optimization calculations, molecular dynamics calculation account for thermal motion.

Molecular dynamics involves conformations, thermodynamic properties and motion of the molecular system and kinetic energy to the potential energy surface. If a set of initial conditions is defined, then Newton's laws cause the molecular system to evolve along a path that is referred to as the molecular dynamics trajectory. This trajectory traverses the potential surface in ways that are of considerable interest to explore. Both the end point of a trajectory and the path taken to get there are of interest in molecular modeling.

Molecular dynamics simulations calculate future positions and velocities of atoms, based on their current positions and velocities (Berendsen, 1990; Karplus and Petsko, 1990). A simulation first determines the force on each atom ( $F_i$ ) as a function of time, equal to the negative gradient of the potential energy (Equation 1) (Berendsen, 1990; Karplus and Petsko, 1990).

$$F_i = -\partial V / \partial r_i \quad (1)$$

where  $V$  = potential energy function and  $r_i$  = position of atom  $i$ . You can then determine the acceleration,  $a_i$ , of each atom by dividing the force acting on it by the mass of the atom (Equation 2).

$$a_i = F_i / m_i \quad (2)$$

The change in velocities,  $v_i$ , is equal to the integral of acceleration over time. The change in the position,  $r_i$ , is equal to the integral of velocity over time. Kinetic energy ( $K$ ) is defined in terms of the velocities of the atoms (Equation 3)

$$K = 1/2 \sum_{i=1}^N m_i v_i^2 \quad (3)$$

The total energy of the system, called the Hamiltonian, is the sum of the kinetic and potential energies (equation 4).

$$H(r, p) = K(p) + V(r) \quad (4)$$

where  $r$  = the set of Cartesian coordinates and  $p$  = the momenta of the atoms.

### Langevin dynamics

Using Langevin dynamics, you can model solvent effects and study the dynamical behavior of a molecular system in a liquid environment. These simulations can be much faster than molecular

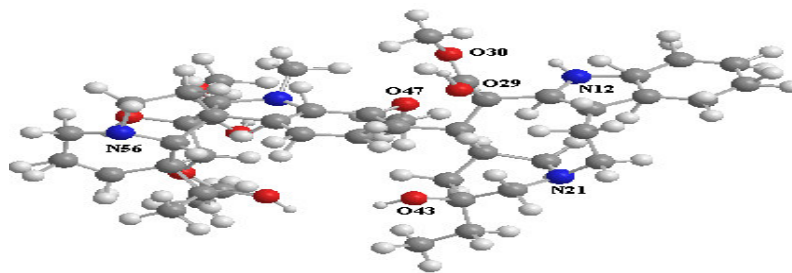


**Figure 1.** Optimized structure of vinblastine.

dynamics. These simulations can be used to study the same kinds of problems as molecular dynamics: time dependent properties of solvated systems at non-zero temperatures. Because of the implicit treatment of the solvent, this method is particularly well-suited for studying large molecules in solution.

Langevin dynamics simulates the effect of molecular collisions and the resulting dissipation of energy that occur in real solvents, without explicitly including solvent molecules. This is accomplished by adding a random force and a frictional force to each atom at each time step. Mathematically, this is expressed by the Langevin equation of motion (Berendsen, 1990; Karplus and Petsko, 1990)

$$a_i = F_i/m_i - \gamma v_i + R_i/m_i$$

Here,  $\gamma$  is the friction coefficient of the solvent, in units of  $\text{ps}^{-1}$  and  $R_i$  is the random force imparted to the solute atoms by the solvent. The friction coefficient is related to the diffusion constant  $D$  of the solvent by Einstein's relation:  $\gamma = k_B T/mD$ . The random force is calculated as a random number, taken from a Gaussian distribution, with an average value of zero and no correlation with the atom's velocity (Mahdavian and Monajjemi, 2010).

### Solvent effect and NMR chemical shift

The electronic structure plays a primary role in determining structure of a molecule. However, changes of the electronic energy associated with a chemical process are comparable, in many cases, with those owed to solvation in solution.

The coupling of continuum models with quantum chemical calculations using SCRF approaches (Tannor et al., 1994; Tomasi and Persico, 1994) has been implemented over the past decade in a number of widely available *ab initio* quantum chemistry program such as Gaussian 98.

To test the influence of the polarized continuum on molecular structure the geometry optimizations were also made in water, methanol and ethanol using self-consistent reaction field (SCRF = dipole) which uses a more reliable cavity as union of a series of interlocking atomic spheres.

Over the past decades the NMR chemical shift measurement in solutions has been applied to a vast range of problems in chemistry and biochemistry and has revealed itself to be an invaluable microscopic probe. It has played an especially important role in the structural understanding of protein owing to its great sensitivity to the environment in which the probing atom is situated. Theories of the chemical shift in solution, on the other hand, have not been well developed owing to the lack of a theory for describing the electronic structure of a solvated molecule.

The gauge including atomic orbitals (GIAO) or applying a "continuous set of gauge transformations (CSGT) are adopted to solve the gauge problem in the calculation of nuclear magnetic shielding (Monajjemi et al., 2008).

The study of chemical shift reveals a serious drawback inherent

in the classical-quantum hybrid approach. The solvent effects on the chemical shift showed temperature dependence opposite to corresponding experimental results. An *ab initio* analysis suggested strongly that the ill behavior is originated from the lack of electron exchange between solute and solvent.

The computations refer to vinblastine molecule, unpolarized by any solvent molecules, whereas the NMR shift measurements were made in water, methanol and ethanol solvents by various dielectric constants, (78.39, 32.63 and 24.55, respectively) (Monajjemi et al., 2007, 2008).

## RESULTS AND DISCUSSION

Direct observation of vinblastine assembled from tubulin has led to a description of microtubules dynamic properties by energy, temperature dielectric constant parameters. Initially, the dynamics of vinblastine was interpreted by theoretical methods of simulation such as Monte-Carlo, molecular dynamic and Langevin force fields.

Defining the relationship between the dielectric constant, temperature and the geometrical structure and optimized energy is central to understanding the mechanism of dynamic modeling by a few force field of simulation.

### Simulation parameters

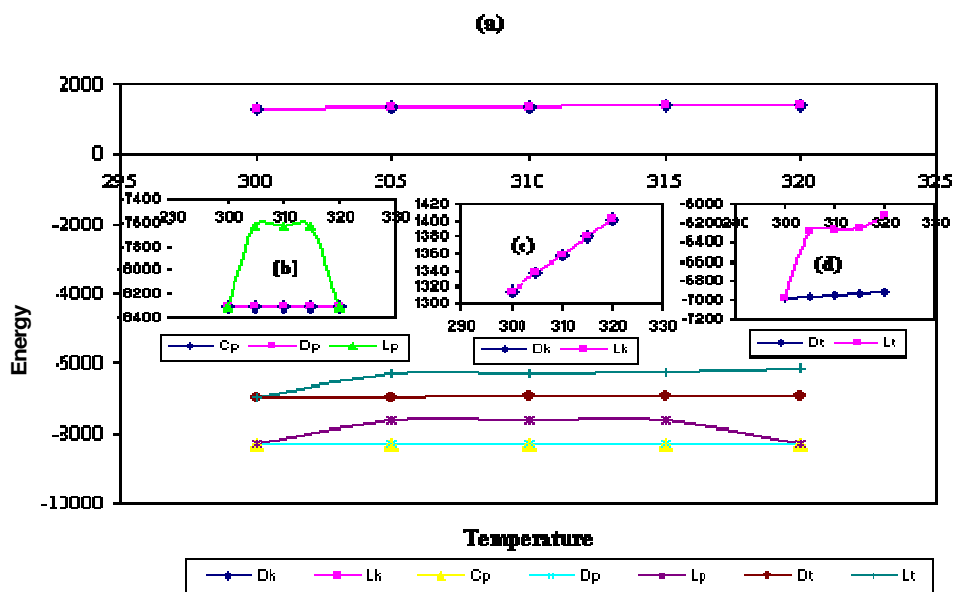
A surprising result of the real-time analysis of vinblastine dynamics was the extent dynamic instability. This is surprising, given their different geometry and optimized properties. The observed behavior must reflect intrinsic properties of the mechanism of dynamic instability and provides useful constraints for the development of mechanistic models.

Study of the solution state has invoked much interest among investigators and a lot has been done in the study of solute-solvent interactions. Water is the main solvent environment for a majority of biomolecules. Within a water medium, the stabilization and operations of biomolecules are not well understood.

In this work, we have determined all possible kinetic, potential and total energy of vinblastine in periodic box of water (Figure 1) by Monte-Carlo, molecular dynamics

**Table 1.** Optimized energies of vinblastine in solution by different force fields at 300 to 320 K.

Temperature(K)	Force Field	$E_{kin}$ (kcal/mol)	$E_{pot}$ (kcal/mol)	$E_{tot}$ (kcal/mol)
300	MC		-8308.08	
	MD	1314.58	-8308.08	-6993.49
	LD	1314.53	-8308.08	-6993.55
305	MC		-8308.08	
	MD	1336.49	-8308.08	-6971.59
	LD	1336.44	-7627.86	-6291.42
310	MC		-8308.08	
	MD	1358.4	-8308.08	-6949.68
	LD	1358.34	-7627.86	-6269.52
315	MC		-8308.08	
	MD	1380.31	-8308.08	-6927.77
	LD	1380.25	-7627.86	-6247.61
320	MC		-8308.08	
	MD	1402.22	-8308.08	-6905.86
	LD	1402.16	-8308.08	-6905.91

**Figure 2.** Investigation of simulated energies (kcal/mol) of vinblastine in solution in a) different force fields b) potential c) kinetic and d) total energies at 300 to 320 K. D = Molecular Dynamic, k = kinetic, C = Monte Carlo p = potential L = Langevin t = total.

and Langevin dynamics at 300,305,310,315,320 K (Table 1, Figure 2).

In Figure 2a has been shown that changes of potential energy vs. temperature in different force fields have more negative values than kinetic and total energies, also by increasing of temperature, stability energy including of potential, kinetic and total energies have been increased.

Although, it has been seen that Langevin dynamics potential has deviation from molecular and Monte-Carlo dynamics potential (Figure 2b). In Figure 2c changes of kinetic energy vs. temperature in all of force field including molecular dynamics, Langevin dynamics and Monte-Carlo simulation are linear and corresponding to each other. Langevin force field for total energy has

deviation from MD, thus MD approach has stabilized energy much more than LD approximation.

In Figure 2d similar to Figure 2b it has been investigated that Langevin dynamics potential has deviation from molecular and Monte-Carlo dynamics potential. Then, in Table 2 the results of calculations with the Onsager model have represented. The comparison between gas (1) and 3, water (78.39), methanol (32.63), ethanol (24.55) with different dielectric constants (gas = 1, water = 78.39, methanol = 32.63, ethanol = 24.55) at three basis sets has shown only a relatively small change of the geometrical parameters for vinblastine structure (Figure 3).

In Figures 3(a, b, c) and (a', b', c') for bond length, bond angle and torsion angle at HF,B3LYP, respectively, the relatively small change in molecular geometry can be understood in terms of the inherent limitation of the Onsager approach for the vinblastine molecule. Therefore, we expect small solvent effects on the charge distributions in comparison to gas phase.

Also, we have seen that optimized geometry coordinates in Figure 3 of O29-C22, O29-C22-O30, O29-C22-O30-C35 and O47-C37-C45-N56 are active points and have indicated the most effect in HF and B3LYP levels.

The possible effects of vinblastine structure have been probed by stabilized energy. In Figure 4a, we have observed that stability energies decrease linearly with increasing of dielectric constants by sto - 3 g(c), 3 - 21 g (d) and 6 - 31 g (e) for HF and (c',d',e') for B3LYP, respectively, also in different biological environment (different solvents), B3LYP/6-31g (d) is better than the other level/basis sets.

It is evident that transfer to a less polar solvent results in a different shift. By plotting the relative energy versus basis sets at various dielectric constants (Figures 4b and b'): It is clear that an increase in the dielectric constants increases the stability of vinblastine.

These curves have many of the same characteristics as the difference between the coordinates of vinblastine in water, methanol and ethanol. The difference spectra, shown in Curves a and b, cannot be due simply to an aggregation of vinblastine molecules, since no difference spectrum was generated under identical conditions between three vinblastine solutions differing.

The results of the above observations strongly suggest that the different curves observed in the vinblastine is predominantly due basis set functions, induced by a change in polarity of the environment.

### Solvent effect on NMR spectra

NMR calculations on vinblastine using Hartree-Fock (HF) and density functional theory (DFT) reveal that methods including electron correlation show significant improvements in the NMR shielding over results.

It might be suggested that optimization of solute molecule in solvent followed by shielding calculations is similar to shielding calculations of solvent  $\pm$  solute as an isolated system. However, if the molecule is first optimized in gas phase and then NMR shielding calculations is performed in the solvent, the solvent  $\pm$  solute interactions are taken into consideration for NMR shielding calculation.

Therefore in solvent effect studies, it is more advisable to carry out shielding calculations in solution even with a fixed (gas and liquid-phase optimized) solute geometry, than to perform shielding computations in vacuo for a solute where the geometry is optimized in solution.

The NMR measurements were carried out using HF,B3LYP/sto-3g,3-21g in GIAO and CSGT methods of nuclear magnetic resonance at theoretical concepts in different dielectric constants (gas, water, methanol and ethanol) (Tables 3a and b).

The results of Tables 3a and b are shown in Figures 5 a and b, where we plot the chemical shift ( $\delta$ ) and chemical shift anisotropy ( $\Delta\sigma$ ) of the vinblastine for each active atoms (N12, N21, O29, O30, O43, O47, N56). We have found that the O29 denoted has maximal shift in all of levels and other indicated atoms almost have the similar shifts in different positions. Also, we have seen that by increasing dielectric constant, value of chemical shift and chemical anisotropy has been increased.

### Conclusion

To conclude, we have performed simulations and solvent NMR of theoretical methodology on vinblastine at constant fields and temperatures 300–320 K by various dielectric constants. In these simulations including Monte Carlo, Molecular Dynamic and Langevin Dynamic methods we have explored many of the structural related aspects of vinblastine. The simulations of vinblastine show that the stabilization energy of vinblastine affects the Monte Carlo force field and increasing of temperature. The best results have gained for potential energy vs. temperature at Monte Carlo force field and by increasing of temperature; stability energy including potential, kinetic and total energies has been increased. In this paper we have presented the theory and implementation of the Onsager model using density functional theory. In our study, we have observed the small changes seen in the reflect of NMR solvent effect theory.

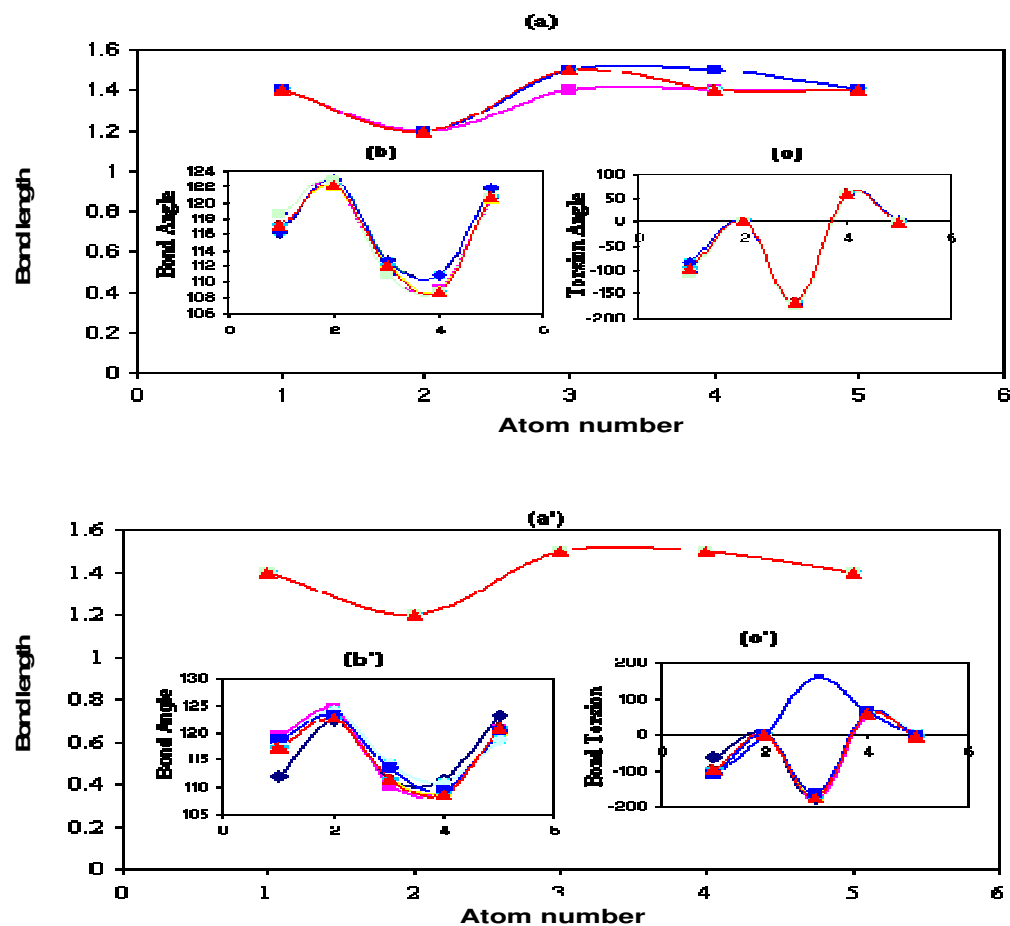
Our calculations have demonstrated that such extrapolation schemes significantly overestimate the vinblastine-to-gas and liquid phases shifts that the O29 was the most active point at indicated structure.

Use of the solutions for characterization of motions and determination of the properties or dynamics of the molecules of interest requires a number of theoretical or computational steps and all of which are current activities of research. Therefore in this paper we summarize the

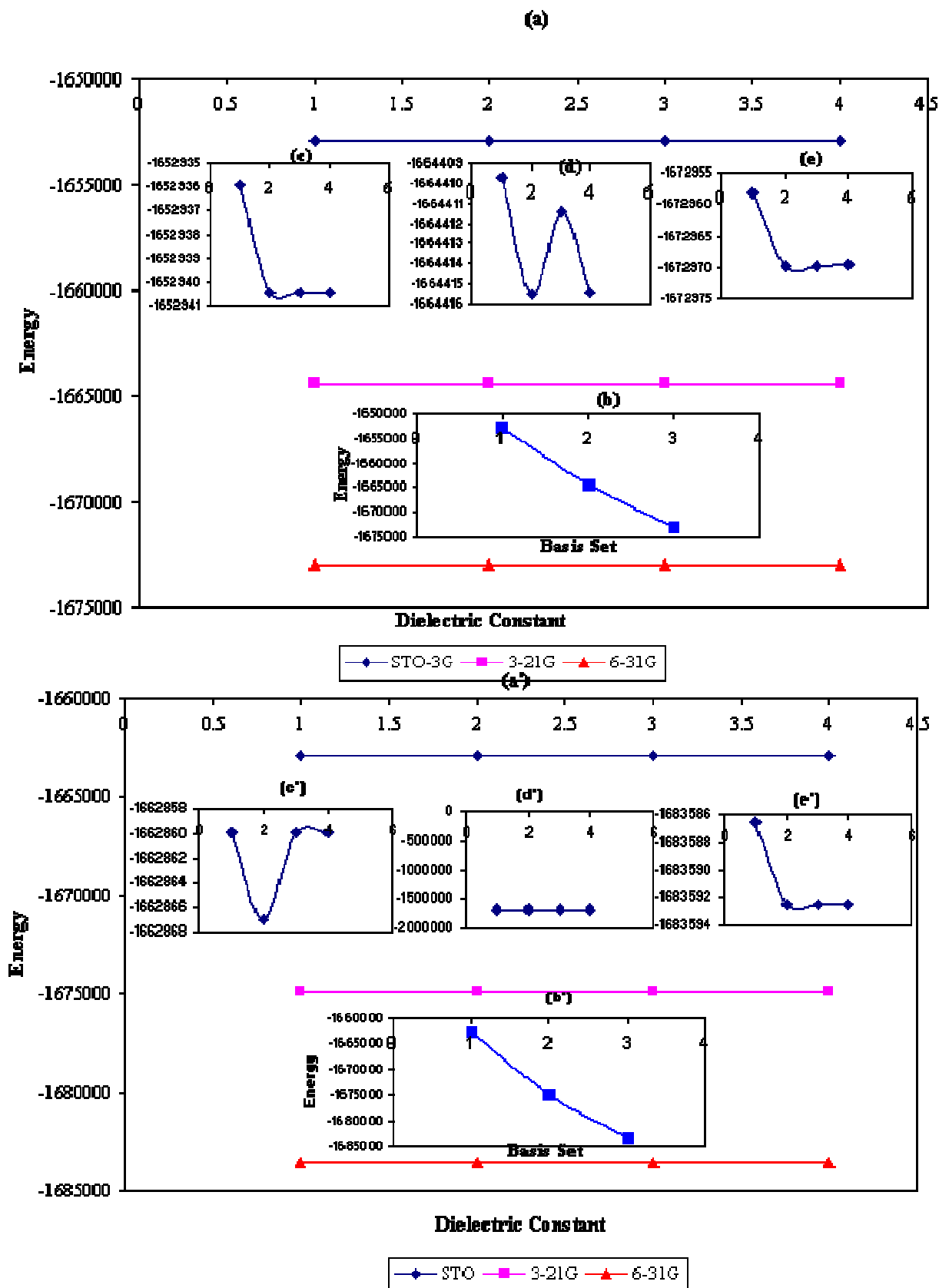


Table 2. cont.

O47-C37-C45	123.2	120.4	120.4	118.7	120.1	120.7	118.7	120.1	120.7	118.7	120.1	120.7
O47-C37-C45-N56	3.8	-1.6	-2.4	5.1	-2.9	-2.3	5.1	-2.9	-2.3	5.1	-2.8	-2.3



**Figure 3.** The curve of optimized geometry coordinates via atom number in (a, b, c) and (a', b', c') for bond length (Å), bond angle (degree) and torsion angle (degree) at HF and B3LYP methods, respectively and comparison between different dielectric constants.



**Figure 4.**(a) Stabilized energies (kcal/mol) of vinblastine structure vs. a) dielectric constant b) basis set c) for sto-3 g d) 3 – 21 g e) 6 - 31g at HF level and (a', b', c' and d') at B3LYP, respectively.

**Table 3(a).** Values of NMR parameters of vinblastine interactions at indicated dielectric constants by **a)** HF **b)** B3LYP methods at two basis sets using GIAO and CSGT approximations.

		$\epsilon$	Sto-3 g						3-21 g				
			$\sigma_{iso}$	$\sigma_{aniso}$	$\eta$	$\delta$	$\Delta\sigma$	$\sigma_{iso}$	$\sigma_{aniso}$	$\eta$	$\delta$	$\Delta\sigma$	
HF	GIAO	1	N12	229.35	42.25	-1.59	8.51	12.77	161.53	52.479	-1.07	16.38	24.57
			N21	318.34	46.00	-0.29	22.25	33.38	277.48	57.477	-0.28	25.00	37.50
			O29	-137.58	882.12	0.34	563.12	844.68	-81.63	660.98	0.03	423.19	634.78
			O30	272.80	148.44	-0.13	-160.06	-240.08	199.61	167.53	-0.23	-176.49	-264.73
			O43	348.75	70.52	-0.51	39.19	58.79	296.06	68.352	-0.52	43.30	64.95
			O47	372.60	98.90	-1.98	-22.65	-33.97	329.29	83.492	-2.26	-20.51	-30.77
		N56	278.66	74.18	0.37	34.99	52.49	232.70	71.441	0.14	32.96	49.45	
		78.39	N12	228.06	41.26	-0.46	9.55	14.33	161.27	53.89	-1.48	18.22	27.33
			N21	303.95	40.44	-1.48	17.32	25.98	278.29	57.41	-0.12	27.23	40.85
			O29	-126.30	868.00	0.42	532.77	799.15	-79.90	657.30	-0.02	429.09	643.63
			O30	276.67	162.30	0.15	-94.75	-142.12	198.63	167.99	-0.25	-178.26	-267.39
			O43	339.48	57.90	-0.15	22.97	34.46	296.37	69.71	-0.32	44.44	66.66
	O47		360.92	84.55	-1.93	-20.30	-30.46	328.67	90.25	-2.40	-21.70	-32.55	
	32.63	N56	266.02	68.84	-0.27	33.51	50.26	232.98	71.49	0.18	35.79	53.69	
		N12	229.55	43.13	-2.19	5.82	8.74	162.06	54.11	-2.52	16.59	24.89	
		N21	318.21	45.91	-0.60	21.69	32.53	277.42	56.32	-0.23	25.94	38.92	
		O29	-137.36	882.81	0.41	560.75	841.12	-81.33	661.20	0.01	424.51	636.77	
		O30	273.16	148.42	0.07	-150.13	-225.20	198.28	168.60	-0.24	-176.45	-264.67	
		O43	348.76	69.26	-0.64	38.13	57.20	296.81	68.41	-0.33	43.43	65.15	
		O47	373.22	99.60	-1.72	-27.27	-40.91	328.78	89.30	-2.40	-22.49	-33.74	
		N56	278.60	73.64	0.14	35.19	52.79	232.82	71.06	0.12	35.68	53.52	
		24.55	N12	229.46	42.42	-2.01	5.71	8.56	161.88	53.72	-1.73	16.89	25.33
			N21	318.21	45.27	-0.74	20.66	30.99	277.93	56.69	-0.19	26.75	40.13
			O29	-136.04	880.30	0.38	573.41	860.12	-79.67	657.54	-0.00	425.03	637.55
O30			273.27	148.33	-0.08	-150.38	-225.57	198.16	168.05	-0.25	-178.30	-267.45	
O43	349.12		67.28	-0.67	35.70	53.55	296.69	68.48	-0.35	43.34	65.01		
O47	372.49		98.30	-1.75	-26.67	-40.01	328.57	90.93	-2.48	-21.66	-32.49		
CSGT	1	N56	278.83	73.81	0.17	34.87	52.30	233.35	70.88	0.14	36.17	54.26	
		N12	105.50	59.828	0.31	20.65	30.98	131.65	80.079	0.13	27.27	40.91	
		N21	150.39	5.1844	-0.51	-2.01	-3.02	237.07	28.036	0.36	8.33	12.49	
		O29	-234.38	681.86	0.16	434.39	651.59	-114.54	582.05	-0.13	371.79	557.69	
		O30	55.65	170.25	-0.19	-189.29	-283.94	131.73	169.09	-0.19	-189.00	-283.50	
		O43	129.38	110.70	0.23	64.71	97.07	214.17	92.216	0.16	60.41	90.62	
		O47	143.95	86.195	0.93	46.35	69.53	247.30	83.947	-1.57	-27.25	-40.88	
		N56	130.59	31.701	-1.79	8.10	12.16	199.62	49.684	-0.56	16.09	24.13	
		78.39	N12	103.59	52.56	0.98	9.94	14.91	131.51	81.55	-0.25	27.73	41.60
			N21	135.14	13.19	-2.82	-3.22	-4.83	237.75	27.53	0.49	8.78	13.18
			O29	-219.14	667.04	0.04	413.85	620.78	-113.51	580.00	-0.17	378.63	567.94
			O30	52.90	177.12	-0.07	-143.27	-214.91	130.78	169.19	-0.18	-187.14	-280.71
	O43		116.07	95.66	0.72	60.46	90.69	214.57	93.24	0.24	62.05	93.08	

Table 3a. Cont'd.

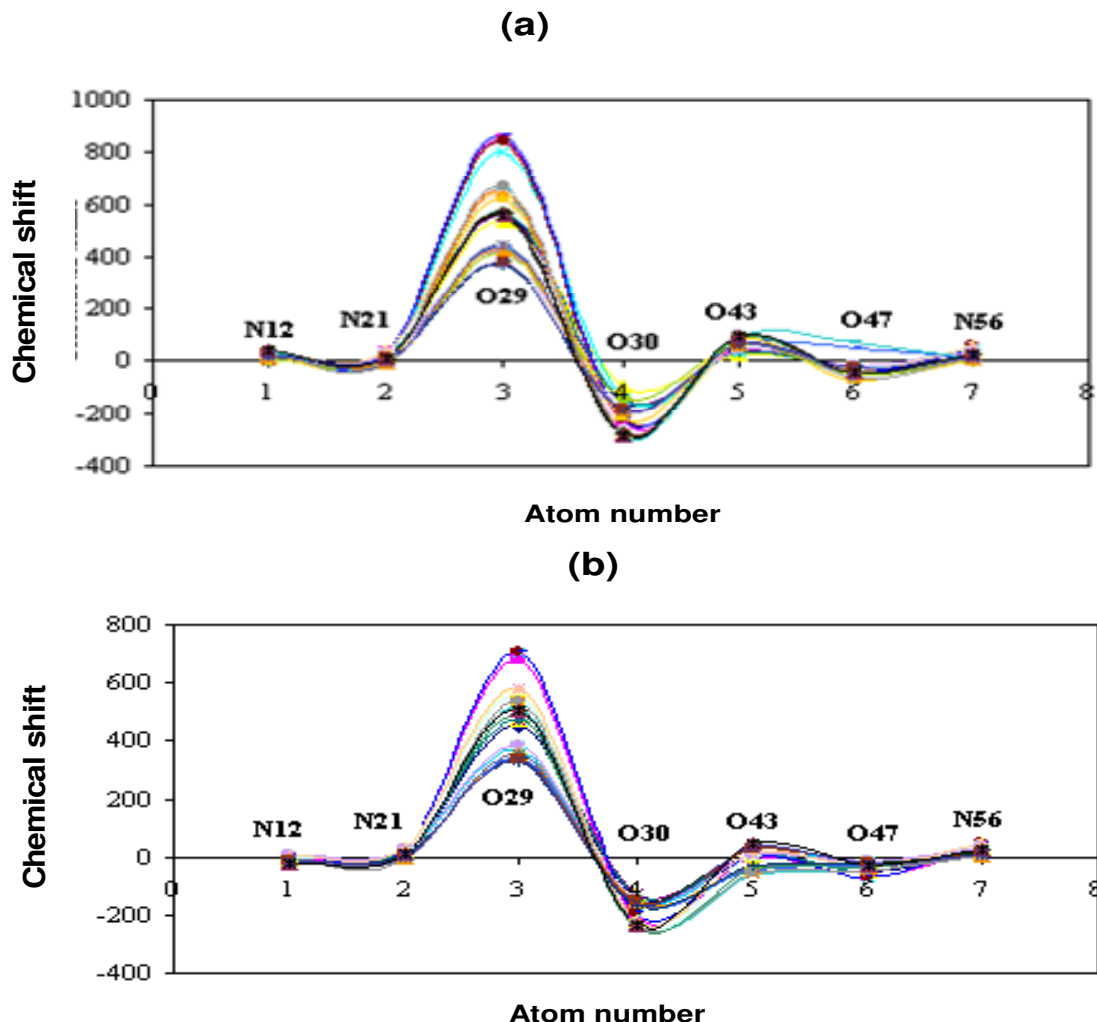
	O47	128.83	79.83	0.48	-48.37	-72.55	246.61	89.77	-1.52	-29.80	-44.70
	N56	118.49	28.82	-2.90	5.53	8.30	199.48	49.22	-0.49	18.09	27.14
32.63	N12	105.58	59.75	0.45	17.68	26.52	132.20	80.61	-0.43	27.36	41.04
	N21	150.45	5.39	-0.58	-2.23	-3.34	237.07	27.25	0.52	7.76	11.64
	O29	-233.89	681.99	0.17	431.43	647.14	-114.18	582.49	-0.16	373.54	560.32
	O30	55.97	170.47	-0.17	-187.84	-281.76	130.60	169.46	-0.19	-188.60	-282.90
	O43	129.32	110.57	0.17	64.73	97.10	214.71	92.94	0.24	61.77	92.65
	O47	144.68	86.21	0.83	-44.47	-66.71	246.62	88.47	-1.63	-30.07	-45.11
24.55	N56	130.47	31.69	-1.30	7.99	11.98	199.29	49.02	-0.48	18.18	27.27
	N12	105.56	60.00	0.61	16.82	25.24	132.07	80.82	-0.35	26.61	39.91
	N21	150.38	5.14	-0.77	-2.11	-3.17	237.47	27.18	0.49	8.25	12.37
	O29	-232.70	680.28	0.14	442.08	663.13	-113.24	580.23	-0.16	374.82	562.24
	O30	56.13	169.95	-0.18	-187.52	-281.29	130.44	168.94	-0.18	-188.12	-282.18
	O43	129.65	109.87	0.20	65.21	97.81	214.91	92.44	0.23	61.46	92.20
	O47	143.97	86.04	0.81	-44.16	-66.24	246.48	90.26	-1.60	-29.85	-44.78
	N56	130.76	31.60	-1.17	8.06	12.09	199.83	48.58	-0.47	18.38	27.57

Table 3b.

		$\epsilon$	Sto-3 g						3-21 g				
			$\sigma_{iso}$	$\sigma_{aniso}$	$\eta$	$\delta$	$\Delta\sigma$	$\sigma_{iso}$	$\sigma_{aniso}$	$\eta$	$\delta$	$\Delta\sigma$	
B3LYP	GIAO	1	N12	207.90	33.96	-0.44	-2.45	-3.68	144.72	39.44	0.44	-2.21	-3.32
			N21	289.29	45.17	-1.63	16.76	25.14	245.57	59.31	-1.04	21.99	32.98
			O29	-48.28	682.01	0.33	452.94	679.41	-34.46	560.56	-0.05	370.96	556.44
			O30	211.31	138.98	0.29	-140.49	-210.74	160.47	140.34	0.05	-159.41	-239.12
			O43	285.11	39.01	-2.40	-1.38	-2.07	248.31	67.75	-0.94	2.95	4.43
			O47	295.60	114.67	-1.17	-48.35	-72.53	269.53	84.45	-2.91	-18.62	-27.94
		78.39	N56	243.35	62.76	0.13	27.35	41.02	195.66	64.93	-0.11	28.08	42.12
			N12	207.63	37.05	-0.80	1.90	2.85	144.19	43.29	-1.38	3.74	5.61
			N21	290.45	44.13	-1.37	17.60	26.40	246.39	58.49	-0.90	22.50	33.75
			O29	-86.74	723.12	0.56	470.37	705.56	-72.18	591.26	0.17	384.67	577.01
			O30	207.81	138.77	0.27	-128.00	-192.00	154.93	154.04	-0.05	-147.13	-220.69
			O43	290.30	40.80	-0.30	4.63	6.95	253.93	70.71	-1.83	6.22	9.34
		32.63	O47	298.40	115.52	-1.03	-48.88	-73.32	272.41	88.22	-2.65	-18.24	-27.36
			N56	247.96	67.21	0.26	29.25	43.88	200.60	68.19	0.075	29.53	44.30
			N12	207.63	37.15	-0.87	1.86	2.79	144.20	43.21	-1.43	3.66	5.50
N21	290.49		44.06	-1.35	17.77	26.65	246.48	58.53	-0.89	22.63	33.95		
O29	-87.29		723.49	0.56	470.67	706.01	-72.52	591.40	0.17	384.83	577.25		
O30	207.86		138.61	0.27	-128.20	-192.30	154.91	153.76	-0.05	-147.34	-221.01		

Table 3b. Continued.

		O43	290.04	40.74	-0.15	4.93	7.39	253.75	71.11	-1.68	6.39	9.59
		O47	298.93	115.57	-1.04	-48.93	-73.40	272.71	88.46	-2.64	-18.33	-27.49
		N56	247.91	67.28	0.26	29.13	43.70	200.57	68.29	0.07	29.44	44.16
	24.55	N12	207.69	36.80	-0.55	2.15	3.23	144.25	42.98	-1.20	3.99	5.99
		N21	290.41	44.11	-1.34	17.69	26.54	246.41	58.51	-0.89	22.58	33.87
		O29	-87.40	723.76	0.55	471.09	706.63	-72.29	591.18	0.16	384.98	577.47
		O30	207.83	138.69	0.24	-130.74	-196.12	154.87	153.71	-0.06	-149.41	-224.11
		O43	290.06	40.37	-0.36	4.90	7.36	253.75	69.84	-1.87	6.56	9.84
		O47	298.85	115.75	-1.03	-48.96	-73.45	272.65	88.56	-2.60	-18.57	-27.86
		N56	247.77	66.96	0.28	28.91	43.37	200.49	68.09	0.09	29.29	43.94
CSGT	1	N12	102.24	45.02	-0.40	-12.70	-19.05	121.86	60.88	-0.33	-15.63	-23.45
		N21	132.05	7.59	-1.98	-1.80	-2.70	213.60	32.74	-0.39	8.61	12.92
		O29	-133.88	512.73	0.14	340.81	511.21	-61.95	491.54	-0.20	325.30	487.96
		O30	20.15	136.30	0.08	-160.11	-240.17	99.97	138.53	0.09	-163.75	-245.62
		O43	72.40	50.73	0.27	-43.15	-64.73	166.13	51.48	0.86	-28.49	-42.74
		O47	86.79	92.08	-1.05	-32.82	-49.23	196.86	92.96	-2.81	-23.75	-35.63
		N56	112.69	24.03	-2.23	3.47	5.20	171.72	43.01	-0.50	13.91	20.87
	78.39	N12	102.11	44.91	0.30	-11.42	-17.14	121.33	60.93	0.46	-13.68	-20.52
		N21	133.49	7.44	-2.77	-1.48	-2.22	214.16	32.32	-0.27	7.82	11.73
		O29	-167.11	549.08	0.36	356.28	534.42	-95.79	515.13	0.01	334.73	502.10
		O30	19.75	138.94	0.03	-155.45	-233.18	96.72	149.12	-0.09	-156.05	-234.08
		O43	78.13	62.97	0.53	-37.09	-55.63	170.92	44.81	0.81	28.99	43.49
		O47	90.64	85.10	-0.69	-34.39	-51.59	198.76	90.00	-2.93	-21.33	-32.00
		N56	115.86	25.86	-1.17	4.79	7.19	175.66	45.44	-0.20	14.86	22.29
	32.63	N12	102.09	44.82	0.29	-11.39	-17.08	121.32	60.75	0.45	-13.60	-20.40
		N21	133.50	7.23	-2.73	-1.49	-2.24	214.24	32.22	-0.24	7.99	11.98
		O29	-167.68	549.31	0.36	356.48	534.72	-96.17	515.31	0.01	334.90	502.36
		O30	19.79	138.83	0.03	-155.58	-233.37	96.68	148.84	-0.09	-156.23	-234.35
		O43	77.80	63.03	0.51	-36.97	-55.46	170.75	44.04	0.83	28.53	42.79
		O47	91.30	84.42	-0.68	-34.46	-51.69	199.16	89.87	-2.94	-21.29	-31.94
		N56	115.83	25.92	-1.18	4.71	7.07	175.64	45.57	-0.20	14.78	22.17
	24.55	N12	102.19	44.80	0.30	-11.60	-17.4052	121.39	60.79	0.46	-13.88	-20.82
		N21	133.39	7.39	-2.82	-1.46	-2.2039	214.13	32.29	-0.27	7.85	11.78
		O29	-167.83	549.63	0.35	356.91	535.3649	-96.06	515.24	0.01	335.14	502.71
		O30	19.84	138.92	0.02	-157.17	-235.762	96.70	148.86	-0.10	-157.75	-236.63
		O43	77.89	62.95	0.53	-37.07	-55.6101	170.66	44.76	0.80	29.02	43.53
		O47	91.23	84.88	-0.66	-34.37	-51.563	199.08	90.06	-2.96	-21.12	-31.69
		N56	115.71	25.67	-1.33	4.50	6.7513	175.56	45.33	-0.20	14.60	21.90



**Figure 5.** Plots of NMR chemical shifts (ppm) of vinblastine interactions vs. different dielectric constants using a) HF b) B3LYP methods corresponding to Table 3.

method and describing the reasons for the choices.

## REFERENCES

- Allan MP, Tildesley DJ (1987). Computer Simulations of Liquids.
- Berendsen WF (1990). H.J.C. Computer simulation of molecular dynamics methodology, applications, and perspectives in chemistry *Angewandte Chemie, International Edition in English*, 29: 992-1023.
- Correia J, Lobert S (2001). Physicochemical aspects of tubulin-interacting antimitotic drugs, *Current Pharmaceutical Design*, 7: 1213-1228.
- Desai A, Mitchison J (1997). A switch in microtubule dynamics at the onset of anaphase B in the mitotic spindle of *Schizosaccharomyces pombe*, *Annu. Rev. Cell Dev. Biol.*, 13: 83-117.
- Haeri HH, Hashemianzadeh SM, Monajjemi M (2009). Temperature effects on the stochastic gating of the ip3r calcium release channel: a numerical simulation study, *J. Biol. Syst.*, 17: 817-852.
- Haile JM (1991). *Molecular Dynamics Simulation*, John Wiley & Sons, pp. 260--267
- Heffington Bunt A (1973). *Investigative ophthalmology*, 12:579-590.
- Jorgensen WL (1988). Biological Reactions Are Slow in Absence of a Catalyst, *Adv. Chem. Phys.*, 70: 469.
- Karplus M, Petsko GA (1990). Molecular dynamics simulations in biology *Nature*, 347: 631-639.
- Leach AR (1996). *Molecular Modeling. Principles and Applications*, Longman.
- Frenkel D, Smith B (2002). *Understanding Molecular Simulations*.
- Lee C, Harrison D, Timasheff N (1975). Interaction of vinblastine with calf brain microtubule protein, *Biological Chemistry*, 250: 9276-9282.
- Lobert S, Correia JJ (2000). Energetics of Vinca Alkaloid Interactions with Tubulin. *Methods Enzymol.*, 323: 77-103.
- Lobert S, Fahy J, Hill T, Duflos A, Etievant C, Correia J (2000). Vinca Alkaloid-Induced Tubulin Spiral Formation Correlates with Cytotoxicity in the Leukemic L1210 Cell Line. *Biochemistry*, 39: 12053-12062.
- Lobert S, Ingram JW, Bridget T, Hill J, Correia J (1998). A comparison of thermodynamic parameters for vinorelbine- and vinflunine-induced tubulin self-association by sedimentation velocity. *Molecular Pharmacology*, 53: 908-915.
- Lobert S, Ingram JW, Correia JJ (1999). Additivity of Dilantin and Vinblastine Inhibitory Effects on Microtubule Assembly, *Cancer Res.*, 59: 4816-4822.
- Lobert S, Ingram JW, Correia JJ (2007). The thermodynamics of vinca alkaloid-induced tubulin spiral formation, *Biophysical Chemistry*, 126: 50-58.
- Lobert S, Vulevic B, Correia J (1996). Energetics of Vinca Alkaloid

- Interactions with Tubulin. Interaction of vinca alkaloids with tubulin: A comparison of vinblastine, vincristine, and vinorelbine, *Biochemistry*, 35: 6806-6814.
- Mahdavian L, Monajjemi M (2010). Alcohol sensors based on SWNT as chemical sensors: Monte Carlo and Langevin dynamics simulation *Microelectronics J.*, 4: 1142-1149.
- Metropolis NA, Rosenbluth AW, Teller AH, Teller E (1953). Equation of state calculations by fast computing machines, *J. Chem. Phys.*, 21: 10-87.
- Monajjemi M, Afsharnezhad S, Jaafari MR, Mirdamadi S, Mollaamin F, Monajem H (2008). Investigation of energy and NMR isotropic shift on the internal rotation Barrier of  $\phi$  dihedral angle of the DLPC: A GIAO study, *Chemistry*, 17: 55-69.
- Monajjemi M, Chahkandi B (2004). Study of the hydrogen bond in different orientations of adenine-thymine base pairs: an ab initio study, *J. Mol. Struct. (THEOCHEM)*, 714: 43.
- Monajjemi M, Heshmat M, Aghaei H, Ahmadi R, Zare K (2007). Solvent effect on  $^{14}\text{N}$  NMR shielding of glycine, serine, leucine, and threonine: comparison between chemical shifts and energy versus dielectric constant, *Bull. Chem. Soc. Ethiopia*, 21: 111-116.
- Monajjemi M, Honarparvar B, Nasser SM, Khaleghian M (2009). nqr and nmr study of hydrogen bonding interactions in anhydrous and monohydrated guanine cluster model: A computational study, *J. Struct. Chem.*, 50: 67-77.
- Monajjemi M, Ketabi S, Hashemian MZ, Amiri A (2006). Simulation of DNA Bases in Water: Comparison of the Monte Carlo Algorithm with Molecular Mechanics Force Fields, *Biochemistry (Moscow)*, 71: 1.
- Monajjemi M, Mahdavian L, Mollaamin F (2008). Characterization of nanocrystalline silicon germanium film and nanotube in adsorption gas by monte carlo and langevin dynamic simulation. *Bull. Chem. Soc. Ethiop.*, 22: 1-10.
- Monajjemi M, Rajaeian E, Mollamin F, Naderi F, Saki S (2008). Investigation of NMR shielding tensors in 1,3 dipolar cycloadditions: solvents dielectric effect, *Phys. Chem. Liquids*, 46: 299-306.
- Monajjemi M, Razavianb MH, Mollaamina F, Naderi F, Honarparvara B (2008). A Theoretical thermochemical study of solute-solvent dielectric effects in the displacement of codon-anticodon base pairs, *Russian J. Phys. Chem. A.*, 82: 113-121.
- Rai S, Wolff J (1996). Localization of the Vinblastine-binding Site on  $\alpha$ -Tubulin, *Biol. Chem.*, 271: 14707-14711.
- Tannor DJ, Marten B, Murphy R, Friesner RA, Sitkoff D, Nicholls A, Ring M, Nalda W, God-dard A, Honig B (1994). Accurate First Principles Calculation of Molecular Charge Distributions and Solvation Energies from Ab Initio Quantum Mechanics and Continuum Dielectric Theory. *J. Am. Chem. Soc.*, 116: 11875-11882.
- Tomasi J, Persico M (1994). Molecular Interactions in Solution: An Overview of Methods Based on Continuous Distributions of the Solvent, *Chem. Rev.*, 94: 2027-2094.
- van Gunsteren WF, Berendsen HJC (1990). Computer simulation of molecular dynamics: methodology, applications and perspectives in Chemistry. *Ang. Chem. Int. Ed.*, 29: 992.
- VanBuren V, Cassimeris L, Odde J (2005). A mechanochemical model for microtubule structure and self-assembly kinetics. *Biophysical J.* 89: 2911-2926.